# In-process Measurement of Micro-Contact Printing

by

Andrés Salgado-Bierman

Submitted to the Department of Mechanical Engineering
in partial fulfillment of the requirements for the degree of

Bachelor of Science in Mechanical Engineering

at the

MASSACHUSETTS INSTITUTE OF TECHNOLOGY

June 2016



Signature redacted

Author .....
Department of Mechanical Engineering
May 23, 2016

Signature redacted

Certified by .....
David Hardt
Professor
Thesis Supervisor

Signature redacted

Accepted by .....
Anette Hosoi
Professor of Mechanical Engineering
Undergraduate Officer

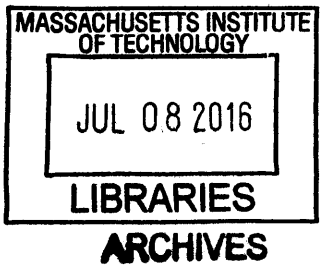

# In-process Measurement of Micro-Contact Printing

by

Andrés Salgado-Bierman

Submitted to the Department of Mechanical Engineering
on May 23, 2016, in partial fulfillment of the
requirements for the degree of
Bachelor of Science in Mechanical Engineering

## Abstract

In micro contact printing, a polymer stamp with sub micron features is use to pattern a substrate. Micro contact printing has many applications including micro machined circuits and miniaturized biological test kits. Success in printing has been achieved in limited batch processing of plate to plate printing. The physics and chemistry of stamp contact and ink transfer has been studied. To make micro contact printing economically viable developments have been made to advance a roll to roll configuration. Roll to roll processing offers the potential of high volume low cost micro manufacturing similar to the high volume achieved by roll to roll processing for traditional lithography. Roll to roll micro contact printers have been built at the lab scale. The process has been demonstrate to have the potential for rapid high volume production. The current limitation is in the quality of the print. Features on the stamp are printed with defects such as breaks or undesired patterning. The source of failure lies with the contact of the stamp; the stamp either breaking contact or collapsing to allow areas outside of the features to make contact. A barrier to better understanding and controlling contact during the printing process has been a lack of in-process measurement. This thesis examines the use of a new optical set-up to monitor stamp contact in-process on a lab level roll to roll micro contact printer. Image based measures of stamp contact quality are presented.

Thesis Supervisor: David Hardt
Title: Professor

# Acknowledgments

I would like to thank professor Hardt for guiding me through this thesis. A special thanks to Maia Bagent for helping me to get to know the lab, and being there whenever I had questions. A final thanks to professor Sang-Gook Kim and the other course instructors of 2.674 for introducing me to principles I applied in my thesis.

# Contents


**1 Introduction** **11**

1.1 Micro Contact Printing and its Applications . . . . . 12

1.2 Stamp Theory and Background . . . . . 14

1.2.1 Material and Deformation . . . . . 14

1.2.2 Failure Modes . . . . . 14

1.3 Roll to Roll Manufacturing . . . . . 15

1.4 Contact Sensing . . . . . 16

**2 Experiment** **18**

2.1 Stamps: Production and Geometry . . . . . 18

2.2 Roll to Roll Aparatus . . . . . 21

2.2.1 Rollers . . . . . 21

2.2.2 Force Control . . . . . 22

2.3 Experimental Set-up, and Data Collection . . . . . 23

2.3.1 Optical Set-up . . . . . 23

2.3.2 Experimental Procedure . . . . . 24

**3 Analysis and Results** **28**

3.1 Range and Resolution of Optical Set-up . . . . . 28

3.2 Identifiable Features . . . . . 28
3.3 Force Versus Deformation . . . . . 30
3.3.1 Failure Modes . . . . . 31

**4 Surrogate Measurements** **33**
4.1 Potential Measurements . . . . . 33
4.2 Inprocess Measurement . . . . . 38

**5 Conclusion** **40**

**6 Appendix** **44**

# List of Figures

1.1 Etched gold features from micro contact printing ; C. Merian, "Development of an Inking System for Continuous Roll-to-Roll Microcontact Printing of Hexadecanethiol (HDT) on Gold-coated PET Substrate," Thesis, Massachusetts Institute of Technology, 2016 . . . . . 13

1.2 Failure modes: (a) Sidewall collapse (b) Roof collapse (c) Buckling (d) Lateral collapse ; J.E. Peterzelka, "Contact region fidelity, sensitivity, and control in roll-based soft lithograpy," Thesis, Massachusetts Institute of Technology, 2012 . . . . . 15

1.3 Two layer black stamp used for imaging: (a) Sketch of stamp construction (b) Image of stamp cross-section ; figure courtesy of Scott Nill . . . . . 17

2.1 Flat stamp casting: (a) Silicon mold (b) Features reproduced in PDMS; J.E. Peterzelka, "Contact region fidelity, sensitivity, and control in roll-based soft lithograpy," Thesis, Massachusetts Institute of Technology, 2012 . . . . . 19

2.2 Patterned drum and cylindrical PDMS stamp with features reproduced; J.E. Peterzelka, "Contact region fidelity, sensitivity, and control in roll-based soft lithograpy," Thesis, Massachusetts Institute of Technology, 2012 . . . . . 20

2.3 Mounting a cylindrical stamp on a roller, scale bar 5 cm: (a) Compressed air lets stamp slide over roller (b) High surface energy keeps stamp adhered to roller; J.E. Peterzelka, "Contact region fidelity, sensitivity, and control in roll-based soft lithograpy," Thesis, Massachusetts Institute of Technology, 2012 . . . . . 21

2.4 Side View of $\mu$Flex Machine: Feed and collection rollers on the left, idler rollers in the middle, glass roller behind camera, force controller and stamp bearing roller on the right; C. Merian, "Development of an Inking System for Continuous Roll-to-Roll Microcontact Printing of Hexadecanethiol (HDT) on Gold-coated PET Substrate," Thesis, Massachusetts Institute of Technology, 2016 . . . . . 22

2.5 Steel Roller on Two Linear Actuators to Control Stamp Contact; C. Merian, "Development of an Inking System for Continuous Roll-to-Roll Microcontact Printing of Hexadecanethiol (HDT) on Gold-coated PET Substrate," Thesis, Massachusetts Institute of Technology, 2016 . . . 23

2.6 Placement of Optical Set-up (a) Impression roller diagram adapted from Adam Libert (b) Optical set-up mounted inside the impression roller, microscope lens looking through the glass . . . . . 24

2.7 Microscope lens behind contact of glass and steel rollers . . . . . 25

2.8 A light source shine through the glass roller from the back side and through the microscope to illuminate the contact. . . . . 26

2.9 A stage allows the set-up to focus and travel vertically. . . . . 27

3.1 Defects in Contact: (left) a large void in the middle of a feature, the black bar in the middle should continue through the photo; (middle) small but complete break in the contact of the middle feature; (right) the middle line in this picture is not completely broken but there are many small breaks in contact . . . . . 29
3.2 Force Versus Deformation . . . . . 31
3.3 Contact Formation (left contact initiation, right narrow feature width as stamp now rests on glass roller) . . . . . 32

4.1 Luminosity Distribution at Different Levels of Contact; levels of applied force increase from left to right . . . . . 35
4.2 Dark Pixel Count Versus Applied Force . . . . . 36
4.3 Edge Crossings and Feature Widths: The left column is for an image of a reasonably good contact. The middle column is a contact disrupted by dust. The right column shows roof collapse. The rows of the figure are as follows from top to bottom: a threshold image of contact; the width distribution of dark horizontal lines (contact); the width distribution of white horizontal lines; the number of threshold crossings per row of the image. . . . . 37
4.4 Luminosity Across a Row of an Image . . . . . 39

# Chapter 1

# Introduction

A goal of the Center for Polymer Microfabrication within the Lab for Manufacturing and Productivity at MIT is to explore the capabilities of micro contact printing. Micro contact printing has numerous applications including creating circuits with fine traces, as well as, miniaturizing biological test kits. Most work in the field has focused on understanding the physics and chemistry of stamp contact and ink transfer, using a plate to plate process. Research in the Center fo Polymer Microfabrication is focused on transferring the lessons learn in plate to plate batch processing to a continuous roll to roll process for micro contact printing. Roll to roll processing shows potential to be able to operate at high rate and high volume, which would reduce costs.

Other students have worked on various aspects of the project ranging from the mechanical design and control of a roll to roll aparatus to the production of novel stamps [1][2][3]. This thesis aims to contribute in the measurement of contact during printing. Stamp contact is a key parameter in determining the quality of the final printed product. Measurement of contact can inform further work on the quality of stamps produced and control of contact in the printing process. This thesis examines

a new optical set-up that is able to measure stamp contact within the roll to roll micro contact printing aparatus. Analysis is presented on what the optical set-up is capable of measuring and how it can be used to inform future work on micro contact printing.

The rest of the introduction covers background on micro contact printing, stamp theory, and roll to roll manufacturing. The thesis then includes a description of the experimental procedures, accompanied by a discussion of the results.

## 1.1 Micro Contact Printing and its Applications

Whitesides and collegues had some of the first publications about microcontact printing in the early 90s [4]. Early printing used a flat plate to plate process. A silicon negative was used to cast a planar PDMS stamp. The silicon mold being fabricated with traditional photolithography. The stamp was inked to print a self asembling mono layer on gold that was later wet etched to reveal the pattern. Etching after micro contact printing has also produced micron scale features in silicon [5].

Micro contact printed arrays can be used to pattern multi-array bio-sensors [6]. Thiébaud et al used micro contact printing to culture cells on micro width lines through the printing of laminin (a protein for the cells to grow on). This was then used in a pdms device for patterned application of micro fluids [7]. Such an approach could be used to miniaturize tests in cell biology.

In its essence micro contact printing uses raised features on a polymer stamp to transfer lines of ink to a surface. In this thesis the simple pattern of parallel lines was used to study stamp contact. Because every featured is essentially a ridge, the lessons

learned from parallel lines will apply to more complex patterns tailored to specific applications. The result of a relatively good printing job looks like this (Figure 1.1). The black lines in the image are gold traces that remain after a wet etch process. The traces were protected from etching by the printing a self assembling mono-layer. Such a result can only come from a high quality stamp contact during printing. The focus of this thesis is on imaging the lines of a stamp as it makes contact and measuring the quality of that contact.

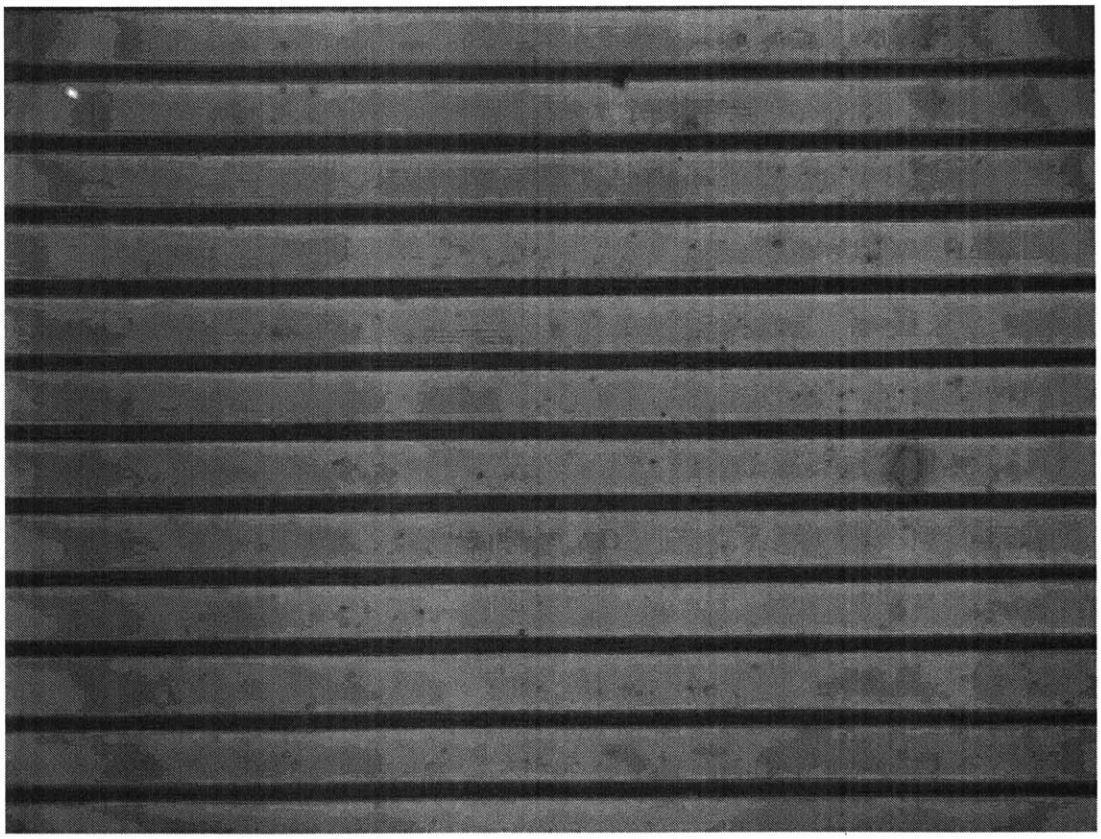

Figure 1.1: Etched gold features from micro contact printing ; C. Merian, "Development of an Inking System for Continuous Roll-to-Roll Microcontact Printing of Hexadecanethiol (HDT) on Gold-coated PET Substrate," Thesis, Massachusetts Institute of Technology, 2016

## 1.2 Stamp Theory and Background

### 1.2.1 Material and Deformation

Polydimethylsiloxane (PDMS) has been the material of choice in the literature for micro contact printing. PDMS is an elastomeric polymer and commonly available as Dow Corning Sylgard 184 product. The elastic modulus is on the order of 1.5Mpa [2]. PDMS has a high surface energy to Young's modulus ratio. Therefore features have a lower risk of adhesion to each other with smaller aspect ratios and placed further apart. PDMS exhibits viscoelastic behavior. Previous analysis of stamp deformation modeled the stamps as purely elastic. Dynamic contact while printing at process speeds may have an impact on feature contact.

### 1.2.2 Failure Modes

The low shear modulus of PDMS leads to conformal contact, but also is the source of the stamp's contact failure modes. Depending on the design of the stamp it may fail in different ways (Figure 1.2). Features with a tall aspect ration make buckle under pressure. Placed close together these features may adhere to one another after failure. The low shear modulus leads to both roof collapse and sidewall collapse. In side wall collapse the sides of a feature deform to make contact with the surface. In roof collapse material from the body of the stamp bulges up to the height of the features, making contact with the printing surface. Models of the critical load for different modes of failure have been expanded into a static model of PDMS stamp load displacement behavior [8].

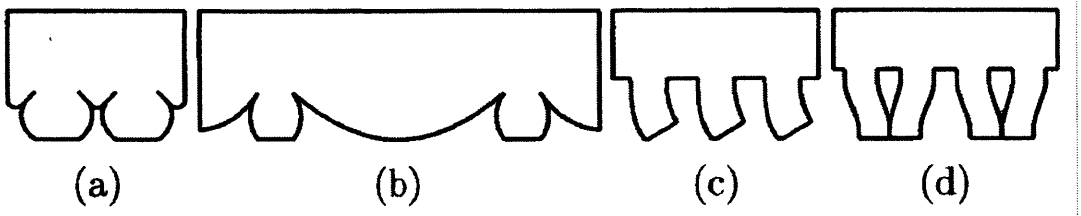


Figure 1.2: Failure modes: (a) Sidewall collapse (b) Roof collapse (c) Buckling (d) Lateral collapse ; J.E. Peterzelka, "Contact region fidelity, sensitivity, and control in roll-based soft lithograpy," Thesis, Massachusetts Institute of Technology, 2012

## 1.3 Roll to Roll Manufacturing

Traditional lithography has been around since the time of the printing press. Roll to Roll printing can be performed on rolls up to 3 meters wide and 2 meters in diameter with production speeds in the order of meters per second [2].

Photo lithography has high resolution and accuracy to create detailed features. However, it is expensive to achieve precision in the alignment of the optics. This leads to a high cost in parts manufactured through photo lithography with costs in the hundreds of dollars per square meter of patterning.

Nano-imprint lithography as well as micro contact printing are two processes that have the potential to offer lower costs than photo lithography. Micro contact printing has the potential to offer high rate production. Micro contact printing has developed from a batch plate to plate process in Whitesides work to a roll to plate, and now a roll to roll process [1]. The key parameter to control in roll to roll processing is the stamp contact.

## 1.4 Contact Sensing

Contact sensing has primarily been performed with microscope imaging. There have been a variety of stamps used and optical set-ups to obtain the images. Initial a prism based approach was used to allow a planar stamp to be loaded vertically [2]. A prism of glass with a flat top and two angled sides was placed over the stamp. Light was direct in through one of the angled faces to reflect off the stamps contact. A camera was situated at the other angled face to capture an image of the contact. The vertical loading allowed study of the load displacement characteristics of the stamp with respect of contact area.

To image stamps on rollers a solid glass cylinder was initially used as one of the rollers. Unfortunately, distortions from the glass prevented quality imaging of the stamp contact. The approach explored in this thesis uses a confocal microscope placed inside a hollow glass roller.

Different stamp technologies have been developed to improve contact imaging. For example, fluorescent stamps [3]. In this thesis a two layer black and clear stamp developed by Scott Nill is used. The features of the stamp are cast from clear PDMS while there is a black pigmented layer below (Figure 1.3). As a side note, the features bear a trapezoidal shape to avoid the failure modes discussed earlier. When imaging the stamp's contact with a glass surface light initially is reflected off the clear layer of the PDMS. When features of the stamp contact the glass the clear PDMS is optically conductive from the glass to the pigmented layer and contacting regions are seen as black through a microscope.

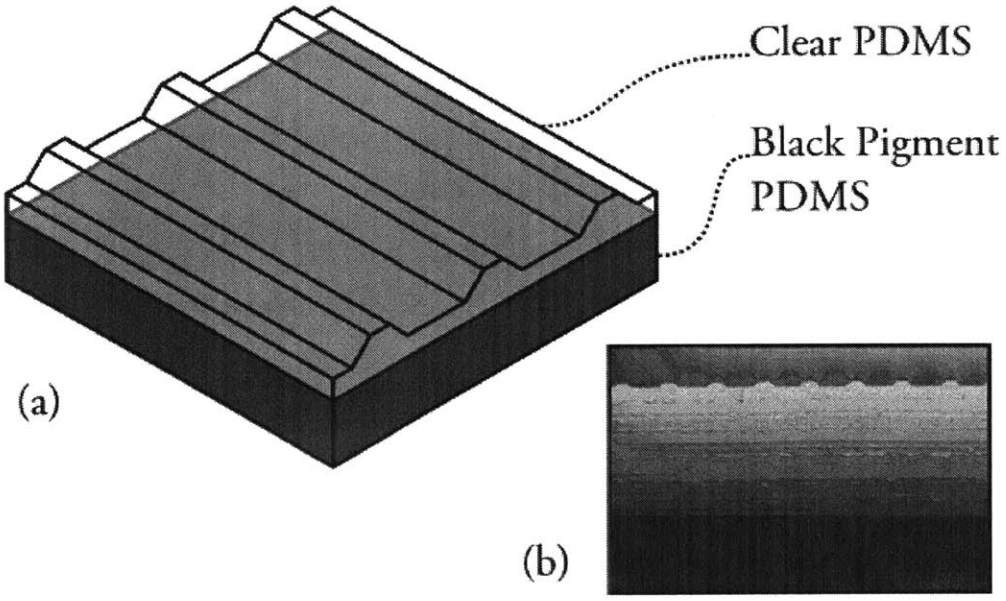


Figure 1.3: Two layer black stamp used for imaging: (a) Sketch of stamp construction (b) Image of stamp cross-section ; figure courtesy of Scott Nill

# Chapter 2

# Experiment

## 2.1 Stamps: Production and Geometry

Initially stamps were formed with silicon originals produced through photo lithography (Figure 2.1). The use of flat stamps in the context of a roll to roll production setting posed two problems. First there would be compressive and tensive stresses along the stamp as it was curved around the roller. Second, there would be a discontinuity where the two ends of the stamp meet on the roller. This discontinuity would cause problems in continuous production.

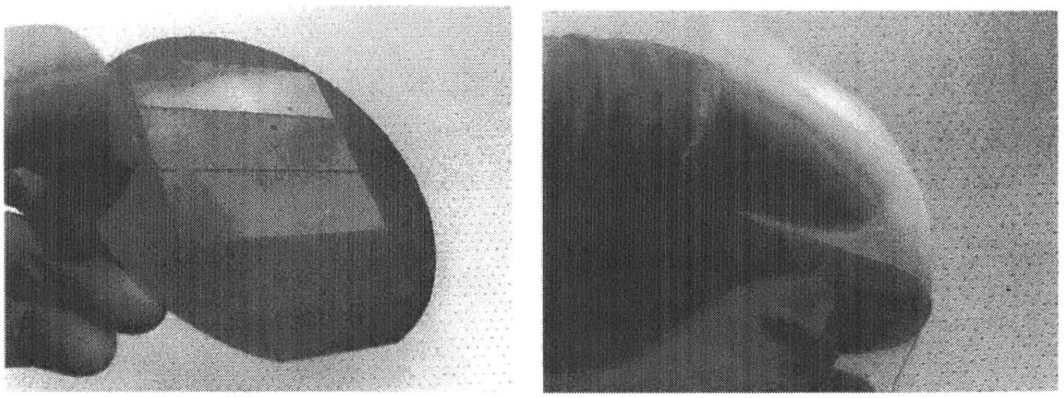

(a) (b)

Figure 2.1: Flat stamp casting: (a) Silicon mold (b) Features reproduced in PDMS; J.E. Peterzelka, "Contact region fidelity, sensitivity, and control in roll-based soft lithograpy," Thesis, Massachusetts Institute of Technology, 2012

A centrifugal casting approach was developed to produce cylindrical stamps custom made for the rollers [9][10]. The production process is still similar. A photo resist and etching is still used to pattern features on the inside of the cylinder (Figure 2.2). PDMS is then placed into the mold and as the cylinder rotates the polymer sets along side the inner edge. To avoid adhesion while mounting cylindrical stamps on a roller an air bushing was developed to guide the stamp onto the roller with out it making direct contact until the stamp was in position (Figure 2.3).

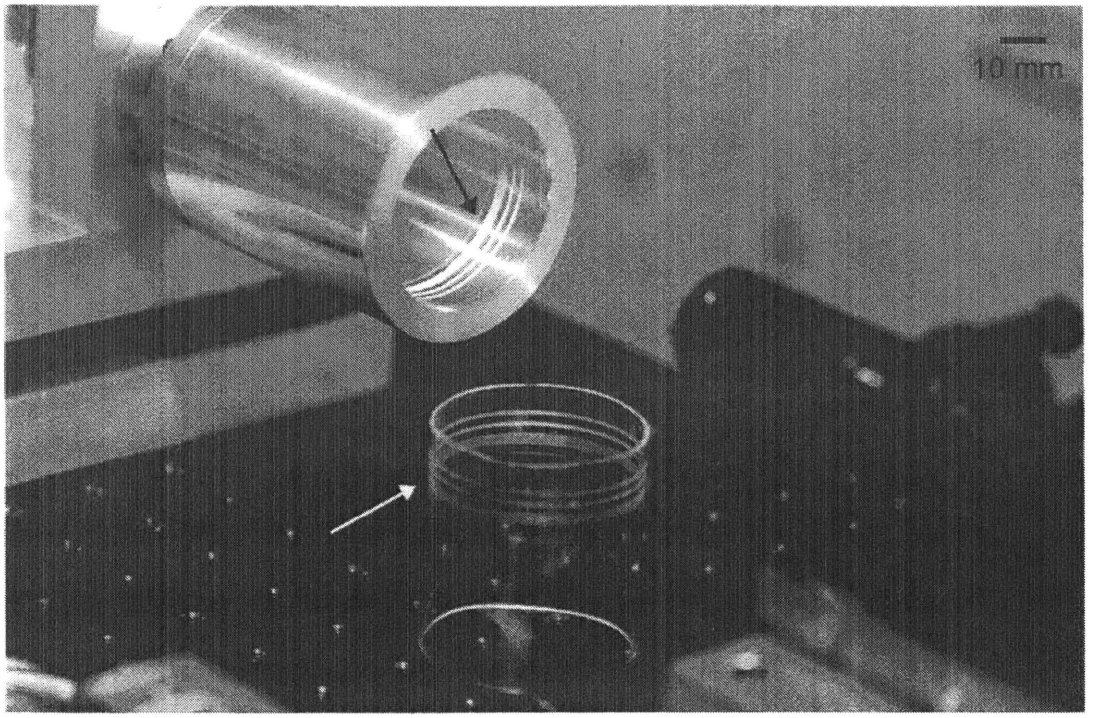


Figure 2.2: Patterned drum and cylindrical PDMS stamp with features reproduced; J.E. Peterzelka, "Contact region fidelity, sensitivity, and control in roll-based soft lithograpy," Thesis, Massachusetts Institute of Technology, 2012

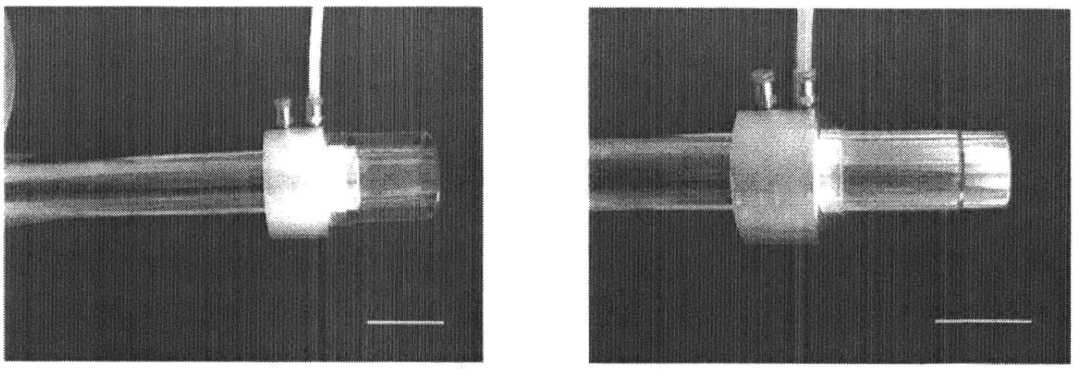

(a) (b)

Figure 2.3: Mounting a cylindrical stamp on a roller, scale bar 5 cm: (a) Compressed air lets stamp slide over roller (b) High surface energy keeps stamp adhered to roller; J.E. Peterzelka, "Contact region fidelity, sensitivity, and control in roll-based soft lithograpy," Thesis, Massachusetts Institute of Technology, 2012

## 2.2 Roll to Roll Aparatus

Because there we no commercial machines suitable for analysis and development of micro contact printing, a roll to roll soft lithography machine was set up in the lab.

### 2.2.1 Rollers

A six roller set up was employed (Figure 2.4). A pair of rollers move the material through the machine. Presently a PET film is used. After the material moving rollers are two idler rollers that guide the PET film onto the glass roller where it would be contacted by the stamp. The material and idler rollers are cantilevered off an aluminum frame. The glass roller is in a supportive frame where three contacts with air bearings on each side of the roller allow it to rotate freely when the machine is in operation.

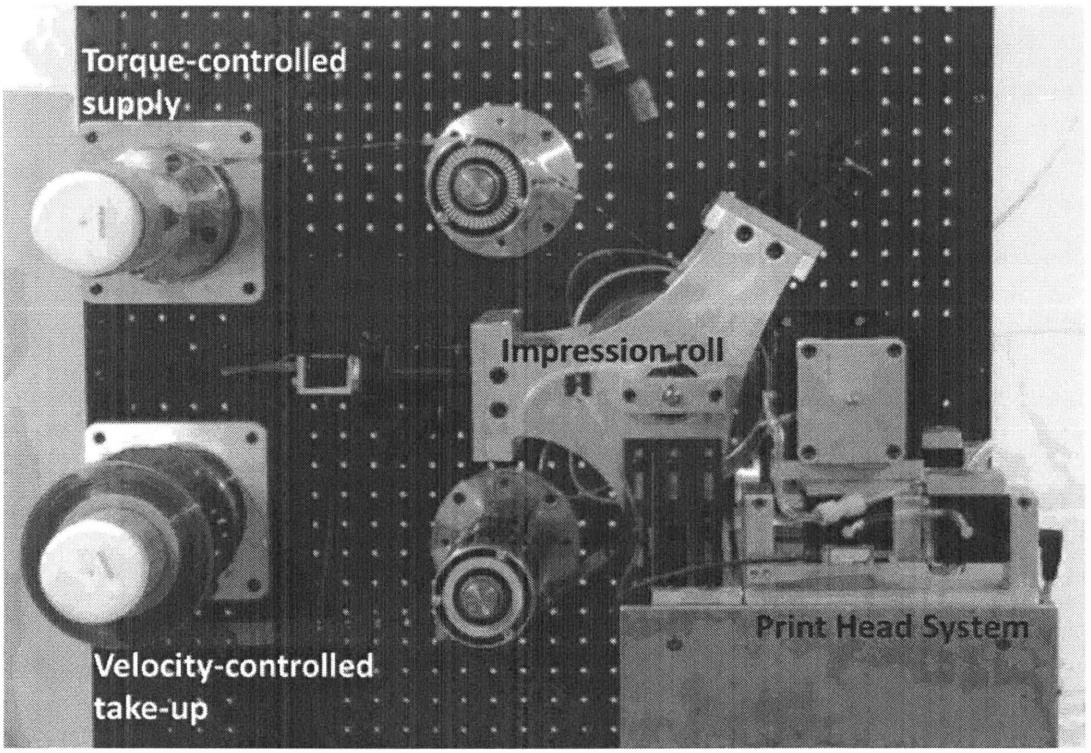


Figure 2.4: Side View of $\mu$Flex Machine: Feed and collection rollers on the left, idler rollers in the middle, glass roller behind camera, force controller and stamp bearing roller on the right; C. Merian, "Development of an Inking System for Continuous Roll-to-Roll Microcontact Printing of Hexadecanethiol (HDT) on Gold-coated PET Substrate," Thesis, Massachusetts Institute of Technology, 2016

### 2.2.2 Force Control

On the same stand that supports the glass roller is an apparatus to control the force with which the stamp makes contact (Figure 2.5). An aluminum roller is supported on two air bearings that are each attached to a linear actuator through a flexure. The flexure allows compliance as the two sides of the roller move relative to each other.

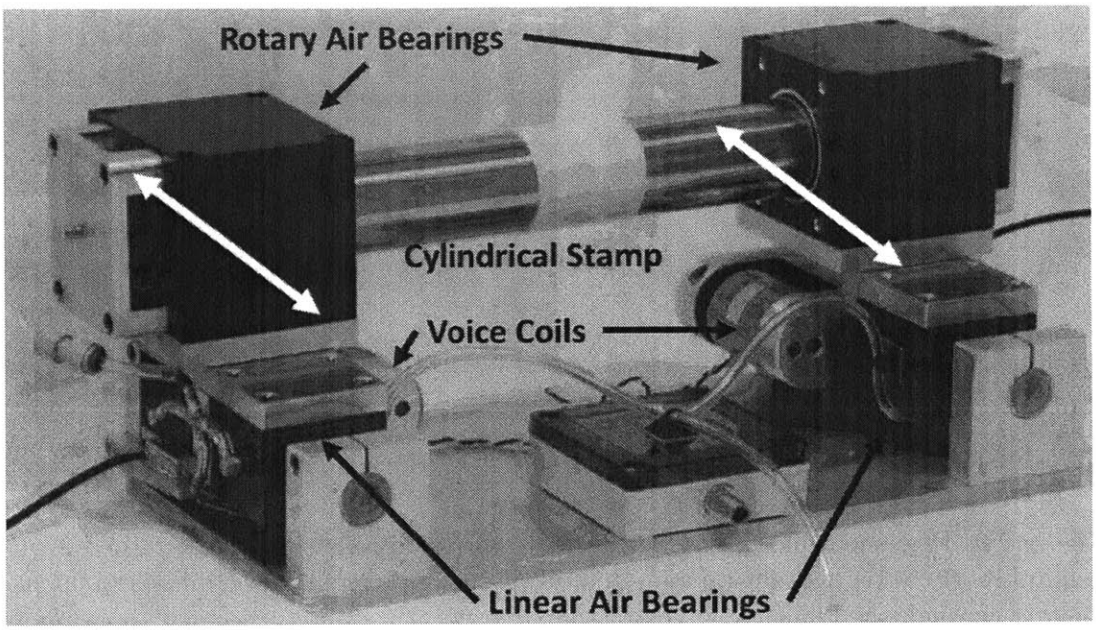


Figure 2.5: Steel Roller on Two Linear Actuators to Control Stamp Contact; C. Merian, "Development of an Inking System for Continuous Roll-to-Roll Microcontact Printing of Hexadecanethiol (HDT) on Gold-coated PET Substrate," Thesis, Massachusetts Institute of Technology, 2016

## 2.3 Experimental Set-up, and Data Collection

### 2.3.1 Optical Set-up

Contact occurs between a steel roller holding the stamp and a larger glass roller. To get a clear image of the contact a hollow glass roller is use, with the optical set-up place inside the cavity (Figure 2.6). A microscope looks through the inside of the glass roller to image contact on the roller's outer surface.

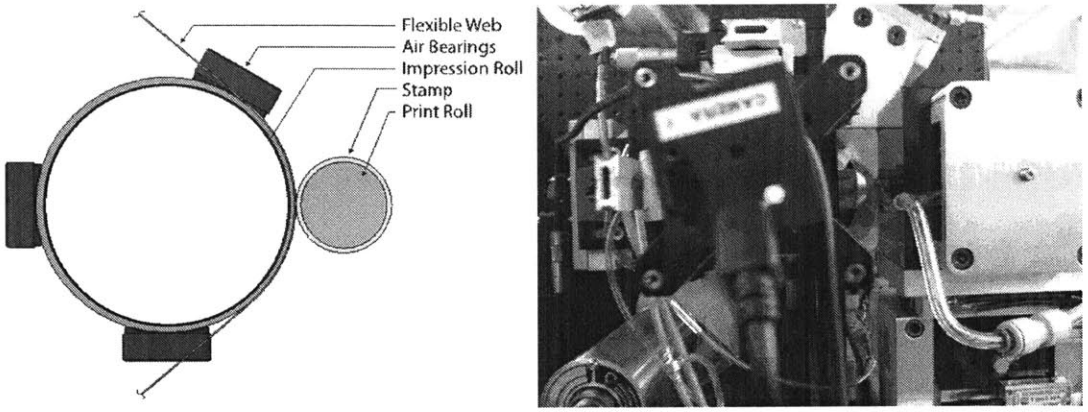


Figure 2.6: Placement of Optical Set-up (a) Impression roller diagram adapted from Adam Libert (b) Optical set-up mounted inside the impression roller, microscope lens looking through the glass

A four times magnification microscope lens was placed inside the roller with a prism behind it (Figure 2.7). Behind the prism and on the outside of the cylinder opposite to the contacting side is a light source (Figure 2.8). The prism let light through to the lens while also reflecting light coming back from the lens onto the camera. The camera and other optics are on a stage that lets the user focus the microscope and travel vertically along the contact region (Figure 2.9).

### 2.3.2 Experimental Procedure

First the stamp had to be cleaned of debris. Isopropyl alcohol was used to avoid moisture in the features after cleaning. Then the stamp was wrapped around the steel roller. One side of the roller was fixed and the other was free to move. This was achieved by detaching the air supply to one of the air bearings. The roller was then put into contact with the glass cylinder by actuating the free side of the roller. Images were taken as the force of contact was varied. A continuous video of the

Figure 2.7: Microscope lens behind contact of glass and steel rollers

contact was taken with uEye Cockpit, a proprietary software supplied by the vendors of the camera used. The voice coils are connected to a closed loop controller run on an FPGA. A virtual instrument in LabView developed by Maia Bageant was used to control current to the voice coil. For analysis, stills were taken from the video of contact.

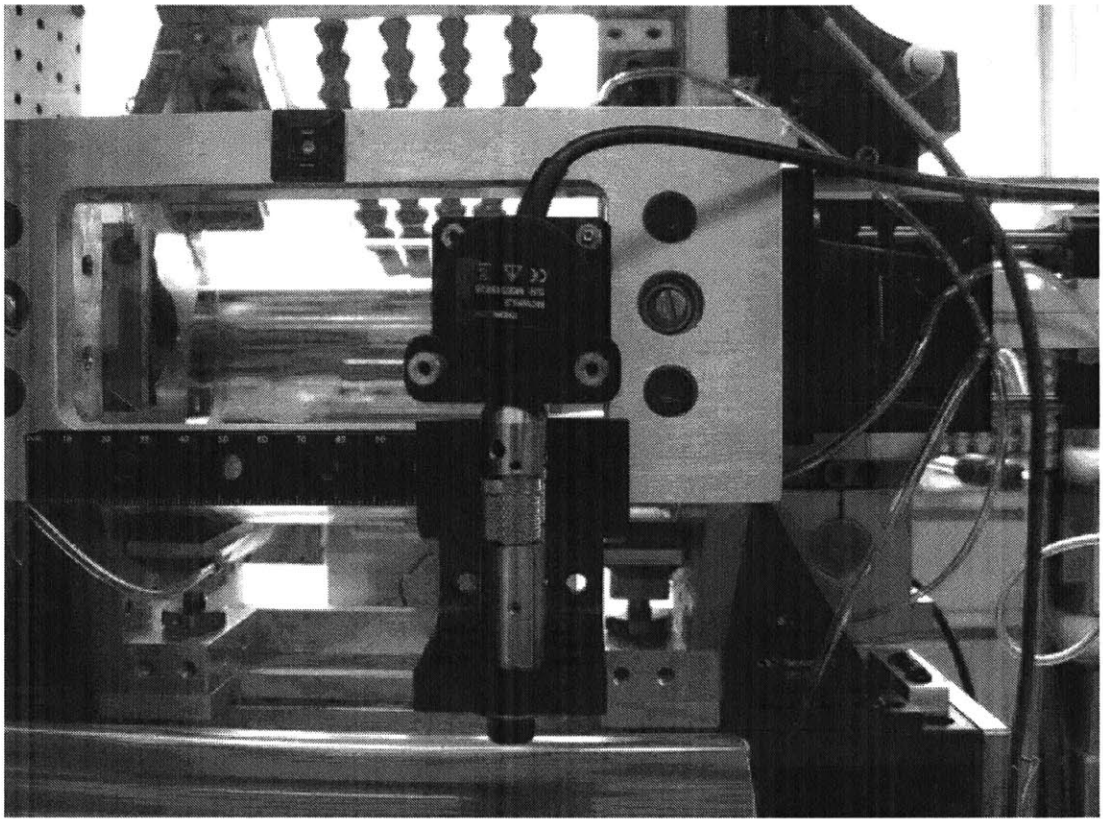

Figure 2.8: A light source shine through the glass roller from the back side and through the microscope to illuminate the contact.

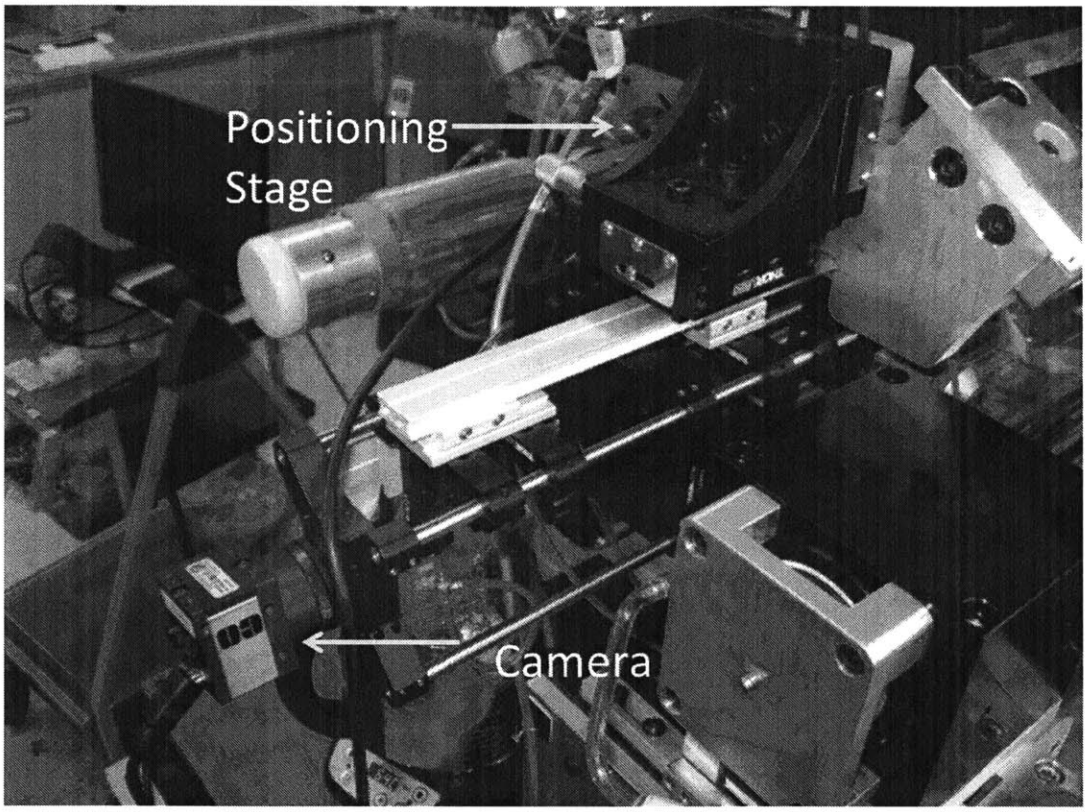


Figure 2.9: A stage allows the set-up to focus and travel vertically.

# Chapter 3

# Analysis and Results

## 3.1 Range and Resolution of Optical Set-up

There is around an inch of travel to focus, and an inch of travel up and down to look at the contact from the top of the roller to the bottom. The set-up is not easily adaptable for transverse motion to image the stamp laterally. The optical rig is clamped in place on rails. Furthermore, there is a confocal light in line with the first lens that must also be moved for proper imaging. The image captured is around 2mm wide spanning 3840 pixels.

## 3.2 Identifiable Features

The optical set-up was able to effectively display contact of the black and clear two layer stamp. As ridges of the stamp made contact with the glass light was able to travel through the transparent upper layer of the PDMS stamp and reflect off the pigmented bottom layer. This formed an image where regions of contact appeared dark, where as regions of the stamp that were not contacting remained lighter in the

image, as light reflected directly of the surface of the top layer of the stamp.

Being able to display regions of contact the optical set-up allowed for features of the stamp to be identified. The main ridges of the stamp pattern can be viewed along with defects in their structure, such as voids and variance in their dimensions (Figure 3.1). Failure modes of partial contact and roof collapse were also captured by the microscope.

Recall figure 1.1 where one can see clear gold lines after etching. To sucessfully create such features we want contact that looks similar. The defects imaged below show where contact deviates from the solid lines we want to create. In the images there is also a gradiation of intensity with dark and light regions. Remember the trapezoidal shape of the stamp as displayed in figure 1.3. The darkest regions are the contacting feature, the lightest regions the roof, and the gradient between them the slanted sidewall.

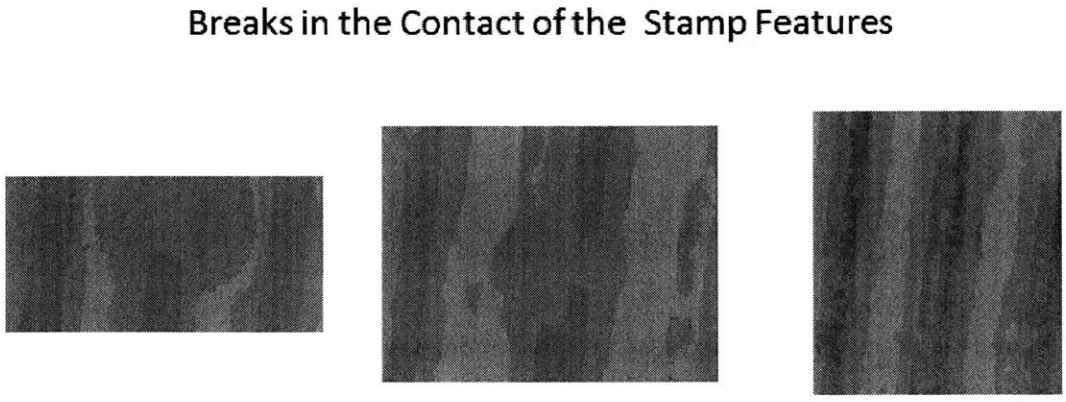


Figure 3.1: Defects in Contact: (left) a large void in the middle of a feature, the black bar in the middle should continue through the photo; (middle) small but complete break in the contact of the middle feature; (right) the middle line in this picture is not completely broken but there are many small breaks in contact

At first glance the breaks in contacts appear to be defects of the stamp, but they are in fact caused by dust particulates on the stamp and printing surface. The presence of the dust is less apparent when it is on the stamp. All that is apparent is breaks in contact once the stamp is against the printing surface. Attributing these defects to imperfections in the stamp would lead one astray in debugging a poor print job. Imaging previously performed by Scott Nill makes it clear that debris is raising the features off the surface and breaking contact. In his imaging dust seen on the printing surface before contact corresponded to areas of broken contact once the stamp was brought against the surface.

What this imaging tells us is that small irregularities of a surface can adversely affect printing. The impact is significant. As seen in the images above a dust particulate is capable of causing a break in the line of a feature. In printing applied to the micro machining of gold circuit traces this would mean the breaking of an electrical connection. The contact defects caused by dust highlight the need to keep printing surfaces and stamps clean, and operate the micro contact printing machine in conditions that allow the printing interface to remain free of debris.

## 3.3 Force Versus Deformation

There is a direct relationship between force applied and the width of the contacting features (Figure 3.2). A least squares linear regression shows the trend. Petrzelka in his thesis on contact region fidelity performed modeling and testing of roll based contact. The preliminary results here are in keeping with the results he obtained and the theory behind stamp contact. This validates the use of the in-process microscope for evaluating the optimal window of contact on the $\mu$flex machine.

The width of contacting features was take from data across the entire image. After some thresholding the width of black lines was measured for every row of pixels in the image. The peak of the resulting distribution was used as the feature width for a given picture after being corrected for the angle of the features in the photo. The angle was measured in imageJ. Force corresponds to the current applied to a voice coil actuating the stamp bearing roller.

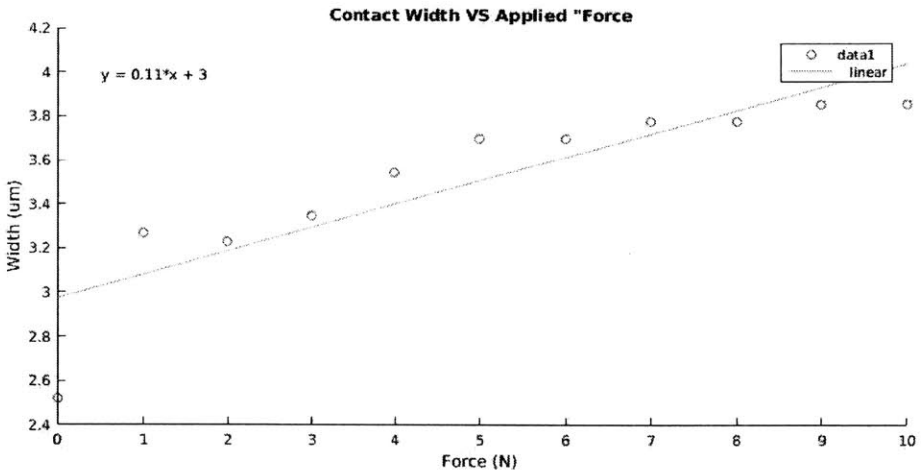


Figure 3.2: Force Versus Deformation

### 3.3.1 Failure Modes

Aside from a failure of stamp contact from a defect in the stamp or debris interfering with the contact, there are the deformation based failure modes of the stamp. One can encounter roof collapse, buckling, or side wall collapse. The stamps being used currently are designed for roof collapse to be the failure mode because this allows a more consistent contact up until failure and coming back from failure.

Roof collapse begins at the center of the stamp's contact with the roller. When imaging for quality control purposes it is possible to miss a failed print if one does

not take the image at the center of the contact.

The other end of contact failure based on applied force is when contact breaks because of too little force (Figure 3.3). When contact is initially made the features have width much narrower than the feature width observed throughout the remaining range of applied force up till roof collapse. As contact is made the feature rapid widens. This is most likely due to a combination of a lowering of the surface energy of the PDMS through adhesion, as well as, the lesser stiffness of the tip of the feature.

The following images of the stamp making contact are stills taken from a video of the stamp making contact with the glass impression roll. The stamp roller was released and let to fall by its own weight into the glass roller. The curves temporarily observed in the shape of the features could potentially be optical irregularity in the glass impression roll or an artifact of the dynamic behavior of the stamp as it makes contact.

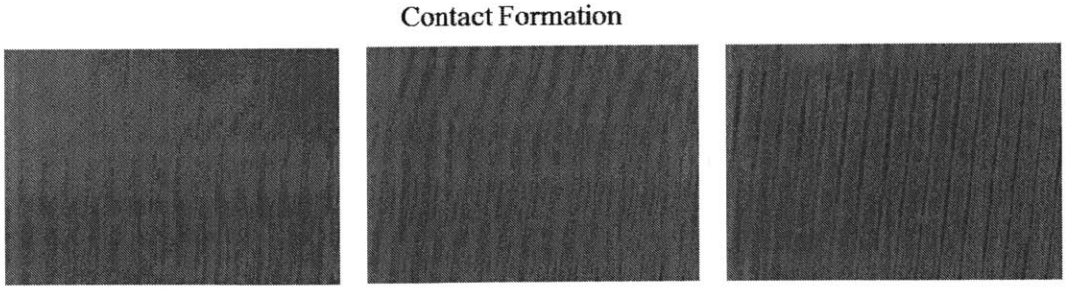


Figure 3.3: Contact Formation (left contact initiation, right narrow feature width as stamp now rests on glass roller)

# Chapter 4

# Surrogate Measurements

## 4.1 Potential Measurements

The goal of any surrogate measurement in the context of the uFlex machine is to quickly relay information about the quality of the contact for either in-process control or in-process quality inspection. When operating the machine in an experimental and non production setting we have as long as we want to perform image processing. However, to look at the quality of contact in-process a quick measure of key parameters is needed. The following chapter discusses some simple algorithms with linear time constants that can produce measures of contact quality.

Intensity distribution was shown to contain information on width of stamp contact. A simple algorithm bins each incoming pixel into one of the 256 values of the 8 bit measure of luminosity. After counting each pixel there is a 256 entry histogram describing the distribution of light intensity across the image. In figure 4.1 one can see three distinct peaks in the distribution for most of the images. The darkest peak corresponds to where the feature contacts the surface. The middle peak corresponds

to the beveled region of the stamp from the top of the feature to the roof. Finally, the lightest region corresponds to the roof.

Thresholding to only count pixels in the darkest peak, there is a clear correlation between the force applied and the number of these darker pixels in the image (Figure 4.1). Again a least squares regression was used to give a linear fit. This relationship is akin to and acts as a surrogate for the relationship between force applied and feature width. The measurement could be used in a feedback controller to adjust the applied force. As well, when the dark pixel count drops significantly it signals the failure mode of breaking contact.

The dark pixel count was calculated by tallying all the pixels in one of the images darker than a certain threshold. The threshold was determined by looking at the local minimum between the darkest peak and the next darkest peak in the intensity distribution.

The remaining operational failure modes are roof collapse and particulate contamination. Again a spike in the number of dark pixels can signal roof collapse, but a second surrogate measurement can confirm the failure mode. With the same threshold one can count edge crossings across a row of the image. Particulates causing broken contact of the stamp raises edge crossing. Similarly as roof collapse creates more vertical lines in the image more edge crossings will be counted.

Whilst keeping track of edge crossing one can keep track of the number of pixels between them and thereby the width of contacting features. While both particulates and roof collapse may cause an increase in the number of edge crossings. The width of features will be more greatly reduced by particulates (Figure 4.3).

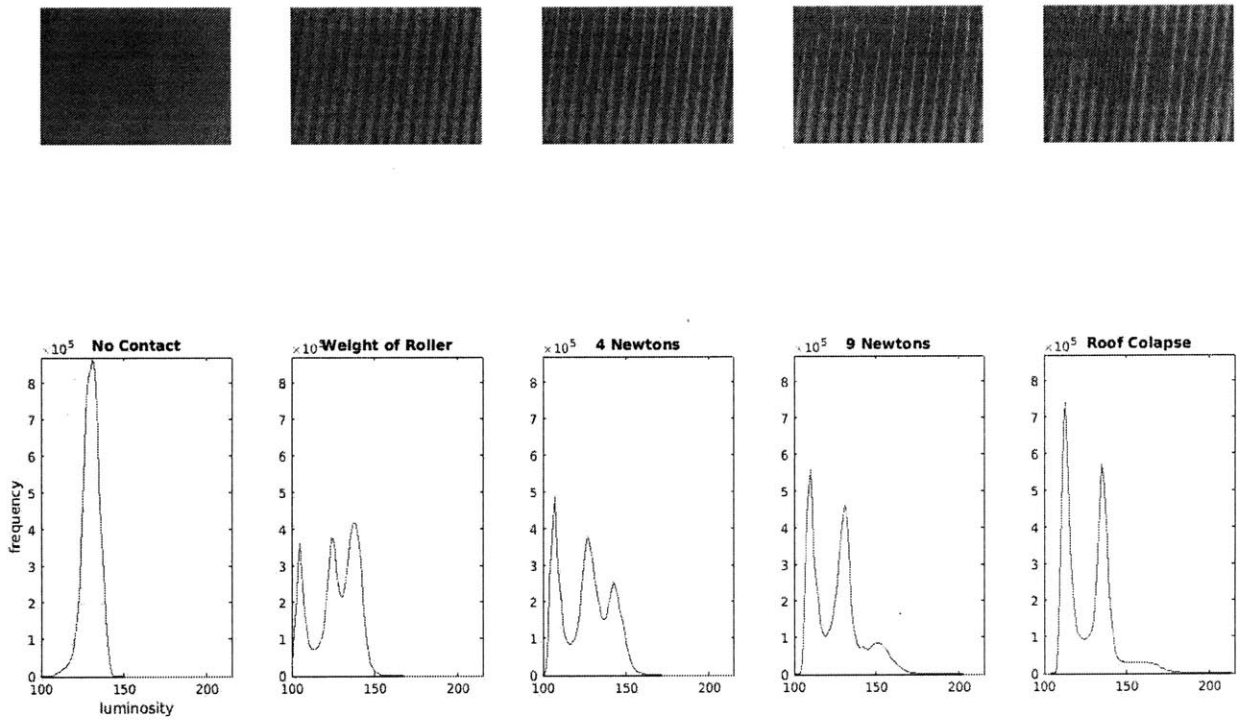


Figure 4.1: Luminosity Distribution at Different Levels of Contact; levels of applied force increase from left to right

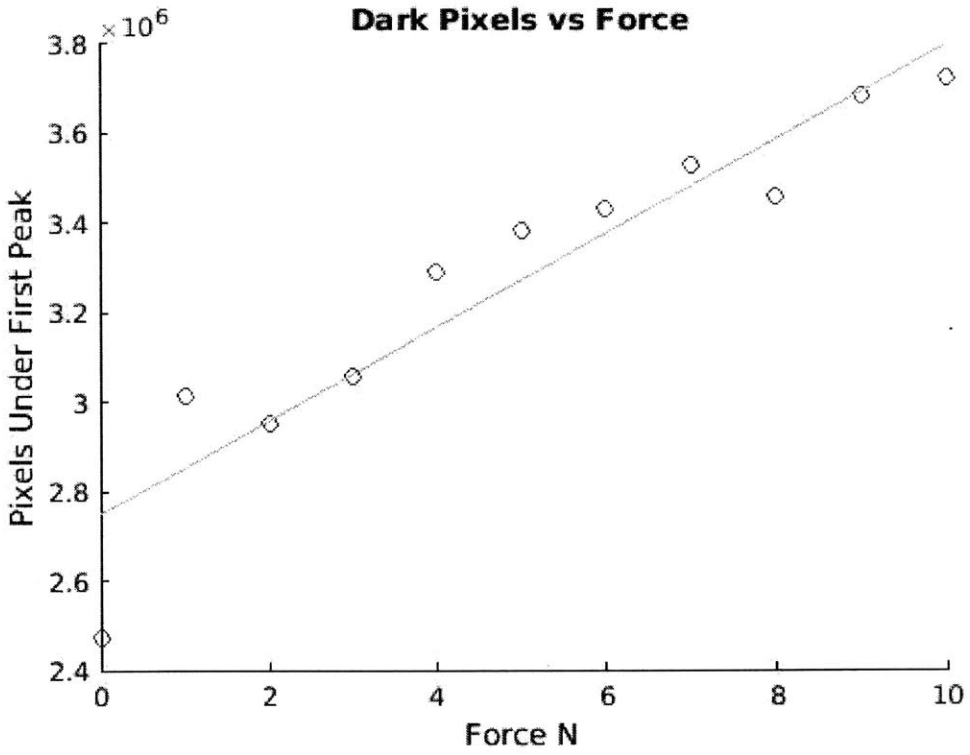


Figure 4.2: Dark Pixel Count Versus Applied Force

Good contact has as expected distinct peak for the width of the black lines of contact and the width of the white spaces in between. When dust starts to cause breaks in the middle of features the distribution flattens considerably. During roof collapse, the peak for white lines moves significantly to the left as the clear space between lines shrinks. In the distribution of dark lines representing contact we see a new peak capturing the contact of the collapsed roof. This addition to the distribution is not as clean as the peak for the features themselves, highlighting the irregularity of contact during roof collapse. The spike close to zero in all the distributions is most likely an artifact of the thresholding. By having a strict cut off in the threshold there are most likely neighboring pixels that just make and just fail to meet the cut off, giving spurious line widths of one or few pixels.

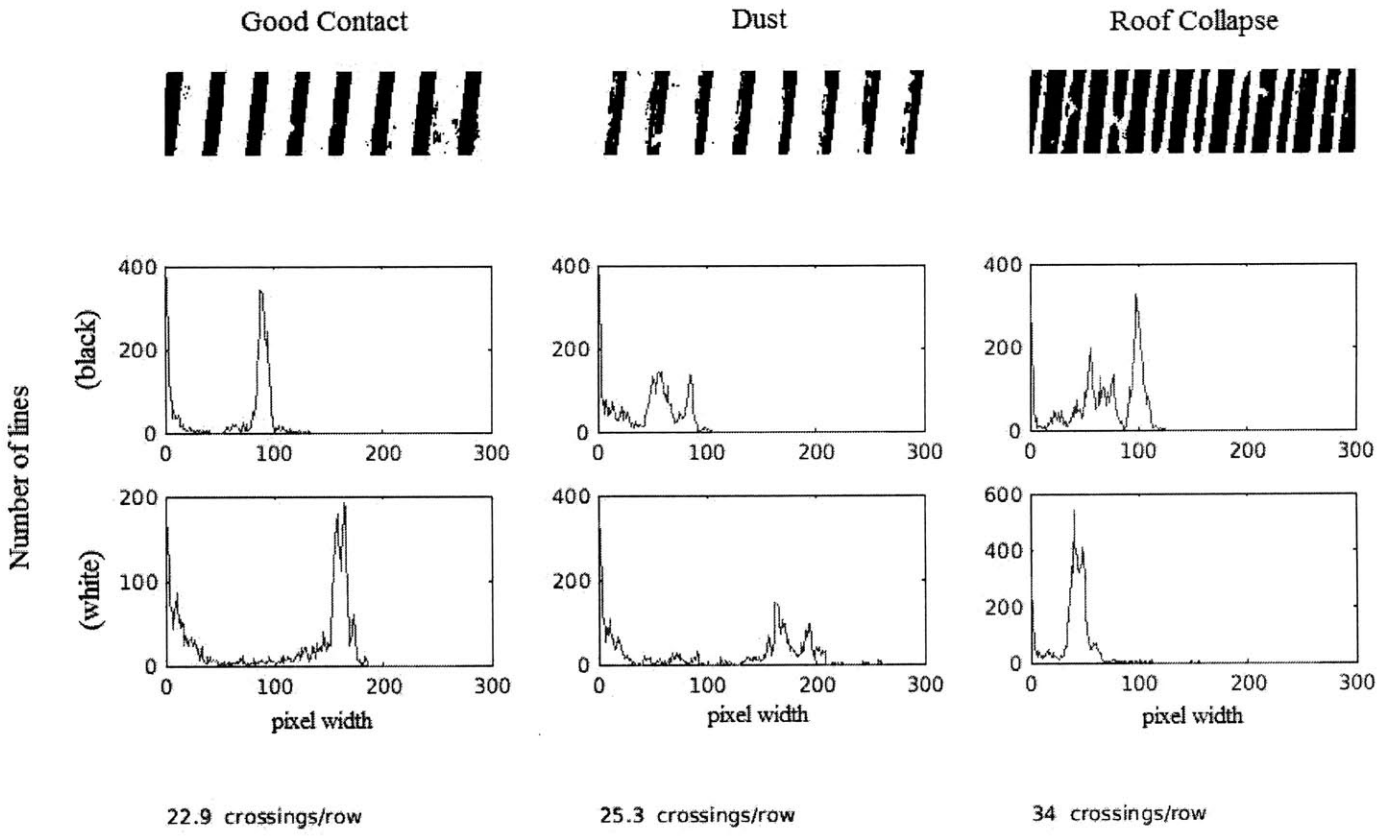


Figure 4.3: Edge Crossings and Feature Widths: The left column is for an image of a reasonably good contact. The middle column is a contact disrupted by dust. The right column shows roof collapse. The rows of the figure are as follows from top to bottom: a threshold image of contact; the width distribution of dark horizontal lines (contact); the width distribution of white horizontal lines; the number of threshold crossings per row of the image.

These three measures of luminosity distribution, edge crossings, and contact width can quickly describe the quality of contact. In addition, the measures can inform which failure mode the contact has entered.

## 4.2 Inprocess Measurement

The chapter above discussed quick measurements of contact quality. This chapters aims to show there is a feasible hardware approach to take such measurements at process speeds. Take for example a high speed camera that captures an 80 by 80 pixel image 500 times a second. If these pixels are sent over an 8-bit data bus, pixels are received at 3.2Mhz. At an FPGA clock speed of 50Mhz there still would be plenty of clock cycles to compare this pixel against an 8 bit threshold reference and add to a count in a register. Furthermore, on an FPGA the measurements discussed above could be calculated in parallel.

With a camera operating at 500 fps, the stamp bearing roller could rotate at 50hz and 10 samples could still be taken per rotation. The ten samples would give a frequency distance significant enough to measure variation in the stamp contact. At 50hz and with a perimeter of around 23cm webbing could move through the machine at productions speeds of 1 meter per second.

The surrogate measurements discussed above were taken studied with a simple feature pattern of straight lines. However, any complicated geometry in a stamped pattern would repeat. As long as you looked at the same chapter of a more complex repeating pattern, intensity, edge crossings, and feature widths would all vary with the quality of contact. Simple optical recognition could ensure that surrogate measurements are taken at the same place in a repeating pattern.

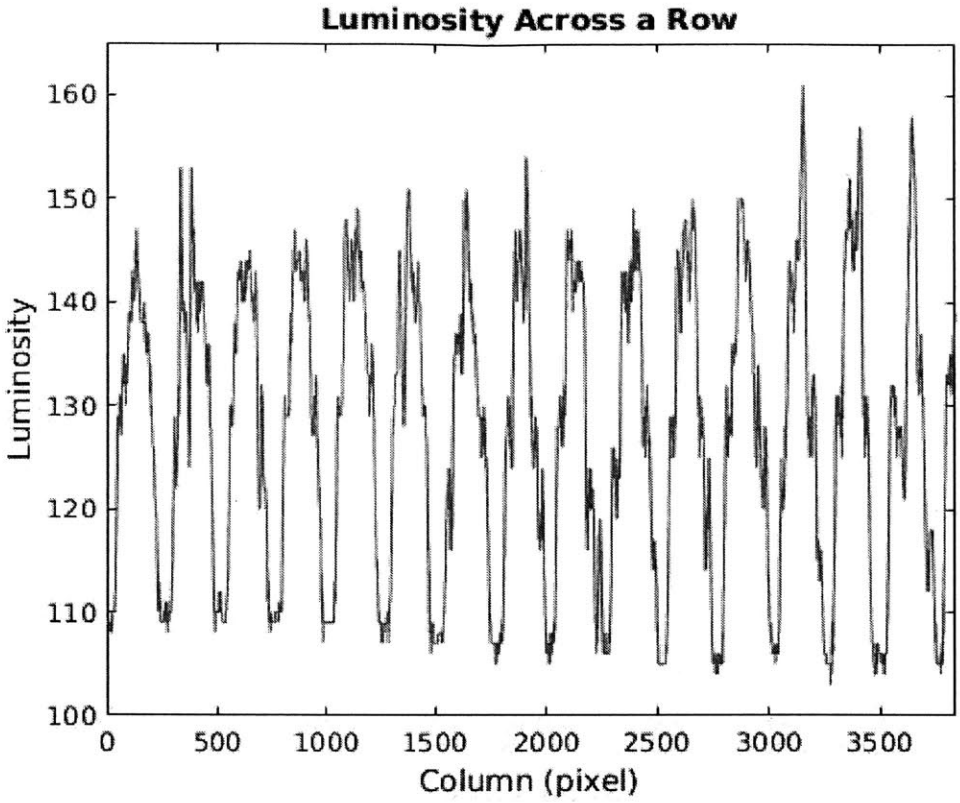


Figure 4.4: Luminosity Across a Row of an Image

Each row of pixels in the image can form a histogram or vector of intensities (Figure 4.4). In a complicated pattern these vectors would vary between rows but repeat. A simple linear classifier could identify a given row. A vector of weights would be doted with the vector of pixels and then compared against a threshold. The threshold would be used to identify a unique row. The weights of the vector could be calculate from a training set of images on a computer and then loaded into memory on an FPGA. The calculation of the dot product could be pipelined in the FPGA with simply a multiplication and addition with each incoming pixel.

# Chapter 5

# Conclusion

It was demonstrated that the optical set-up can image contact and its defects. Though it may seem trivial dust was a source of many defects. The production approach to any successful micro contact printer must consider how to keep printing surfaces clean. Further work can be done to model the dynamic load displacement behavior of the PDMS stamps. Surrogate measurements were identified to indicate the quality of stamp contact. The tally of pixels over a threshold in the image proved to be a surrogate for deformation of contacting features and load applied. Threshold crossings per row were show to indicate breaks in a feature as well as roof collapse. The width distribution of features informed degree of contact and failure modes.

An approach to real time image processing for force or quality control was discussed. Future projects can develop the image processing approach. There is additional work to be done in studying imaging with a substrate in place, as well as, with inked stamps.

One of the limitations of this work was that it looked at contact with glass, where as during printing contact shall be with the PET substrate. When looking through

the glass to a stamp contacting the PET it was not possible to focus on the contact. Instead only the back side of the PET came into view. A potential solution to this problem to attempt in future work would be to have a clear layer of PDMS between the glass and the PET film. Both the glass and the PET are transparent, but because of their interface we can not clearly see through the two layers. Because of PDMS' high surface energy it could make conformal contact between the PET and the glass impression roll, forming an optically conductive interface, allowing the microscope to see through to the surface of the PET.

# Bibliography


[1] Scott Nill. "integrated hardware, software, and sensor design for control of a scalable, continuous roll-to-roll microcontact printing process". Master's thesis, Massachusetts Institute of Technology, 2014.

[2] Joseph E Petrzelka. *"Contact region fidelity, sensitivity, and control in roll-based soft lithography"*. PhD thesis, Massachusetts Institute of Technology, 2012.

[3] Larissa F Nietner, Scott T Nill, David E Hardt, Muhammad A Hawwa, Hassen Ouakad, and Hussain Al-Qahtani. Fluorescent contact imaging for in-process print sensing, January 30 2015. US Patent App. 14/609,925.

[4] Amit Kumar and George M Whitesides. Features of gold having micrometer to centimeter dimensions can be formed through a combination of stamping with an elastomeric stamp and an alkanethiol âĂŸâĂŸinkâĂŹâĂŹfollowed by chemical etching. *Applied Physics Letters*, 63(14):2002–2004, 1993.

[5] Younan Xia, Milan Mrksich, Enoch Kim, and George M. Whitesides. Microcontact printing of octadecylsiloxane on the surface of silicon dioxide and its application in microfabrication. *Journal of the American Chemical Society*, 117(37):9576–9577, 1995.

[6] Milan Mrksich and George M Whitesides. Patterning self-assembled monolay-

ers using microcontact printing: a new technology for biosensors? *Trends in biotechnology*, 13(6):228–235, 1995.

[7] Pierre Thiébaud, Lars Lauer, Wolfgang Knoll, and Andreas Offenhäusser. Pdms device for patterned application of microfluids to neuronal cells arranged by microcontact printing. *Biosensors and bioelectronics*, 17(1):87–93, 2002.

[8] Joseph E Petrzelka and David E Hardt. Static load-displacement behavior of pdms microfeatures for soft lithography. *Journal of Micromechanics and Microengineering*, 22(7):075015, 2012.

[9] Joseph E Petrzelka and David E Hardt. Laser direct write system for fabricating seamless roll-to-roll lithography tools. In *SPIE MOEMS-MEMS*, pages 861205–861205. International Society for Optics and Photonics, 2013.

[10] Larissa F Nietner and David E Hardt. Direct-write photolithography for cylindrical tooling fabrication in roll-to-roll microcontact printing. *Journal of Micro and Nano-Manufacturing*, 3(3):031006, 2015.

# Chapter 6

# Appendix

Included in this section are the Matlab scripts used to analyze microscope images, as well as, generate figures.

This function generates the intensity histogram.

```
peaks = zeros(11,1);

for n = 0:10
[histo, img] = inhisto((strcat(num2str(n),'n.png')));
for p = 100:117
peaks(n+1) = peaks (n+1) + histo(p);
end
end

x = [0:10];
figure
plot(x,peaks)
```

This script generates the luminosity distribution figure.

```
peaks = zeros(11,1);

for n = 0:10
[histo, img] = inhisto((strcat(num2str(n),'n.png')));
for p = 100:117
peaks(n+1) = peaks (n+1) + histo(p);
end
end

x = [0:10];
figure
plot(x,peaks)
```

This script generates the dark pixels versus force figure.

```
peaks = zeros(11,1);

for n = 0:10
[histo, img] = inhisto((strcat(num2str(n),'n.png')));
for p = 100:117
peaks(n+1) = peaks (n+1) + histo(p);
end
end

x = [0:10];
figure
```

```
plot(x,peaks)
```

This function mades an image black and white based on a threshold.

```
c_debris = 0;
c_qual = 0;
c_roofcolapse = 0;
for i = 1:2000
c_debris = c_debris + 2*d_debris(i);
c_qual = c_qual + 2*d_qual(i);
c_roofcolapse = c_roofcolapse + 2*d_roofcolapse(i);
end


c_debris = c_debris/476;
c_qual = c_qual/476;
c_roofcolapse = c_roofcolapse/476;
```

This function calculates line widths from a thresholded image.

```
c_debris = 0;
c_qual = 0;
c_roofcolapse = 0;
for i = 1:2000
c_debris = c_debris + 2*d_debris(i);
c_qual = c_qual + 2*d_qual(i);
c_roofcolapse = c_roofcolapse + 2*d_roofcolapse(i);
end
```

```
c_debris = c_debris/476;
c_qual = c_qual/476;
c_roofcolapse = c_roofcolapse/476;
```

This script calculated the number of edge crossings per row.

```
c_debris = 0;
c_qual = 0;
c_roofcolapse = 0;
for i = 1:2000
c_debris = c_debris + 2*d_debris(i);
c_qual = c_qual + 2*d_qual(i);
c_roofcolapse = c_roofcolapse + 2*d_roofcolapse(i);
end
```

```
c_debris = c_debris/476;
c_qual = c_qual/476;
c_roofcolapse = c_roofcolapse/476;
```

This script generated the figure comparing egdge crossings and line widths.

```
debris_str = [num2str(c_debris, 3), '  crossings/row'];
qual_str = [num2str(c_qual, 3), '  crossings/row'];
roofcolapse_str = [num2str(c_roofcolapse, 3), '  crossings/row'];

x = [1:265];
```

```
figure
%top row pictures
subplot(4,3,1)
imshow(bw_qual)
%
subplot(4,3,2)
imshow(bw_debris)
%
subplot(4,3,3)
imshow(bw_roofcolapse)
%
% 2nd row dark plots 4-6
subplot(4,3,4)
plot(x,d_qual(1:265))
%title('Desired Contact')

subplot(4,3,5)
plot(x,d_debris(1:265))
%title('Debris')
subplot(4,3,6)
plot(x,d_roofcolapse(1:265))
%title('Roof Collapse')


% 3rd row light plots 7-9
```

```
subplot(4,3,7)
plot(x,w_qual(1:265))
subplot(4,3,8)
plot(x,w_debris(1:265))
subplot(4,3,9)
plot(x,w_roofcolapse(1:265))


% 4th row crossings per row 10-12

ax = subplot(4, 3, 10);
text(0,0.5,qual_str);
set ( ax, 'visible', 'off')

ax2 = subplot(4, 3, 11);
text(0,0.5,debris_str);
set ( ax2, 'visible', 'off')

ax3 = subplot(4, 3, 12);
text(0,0.5,roofcolapse_str);
set ( ax3, 'visible', 'off')
```